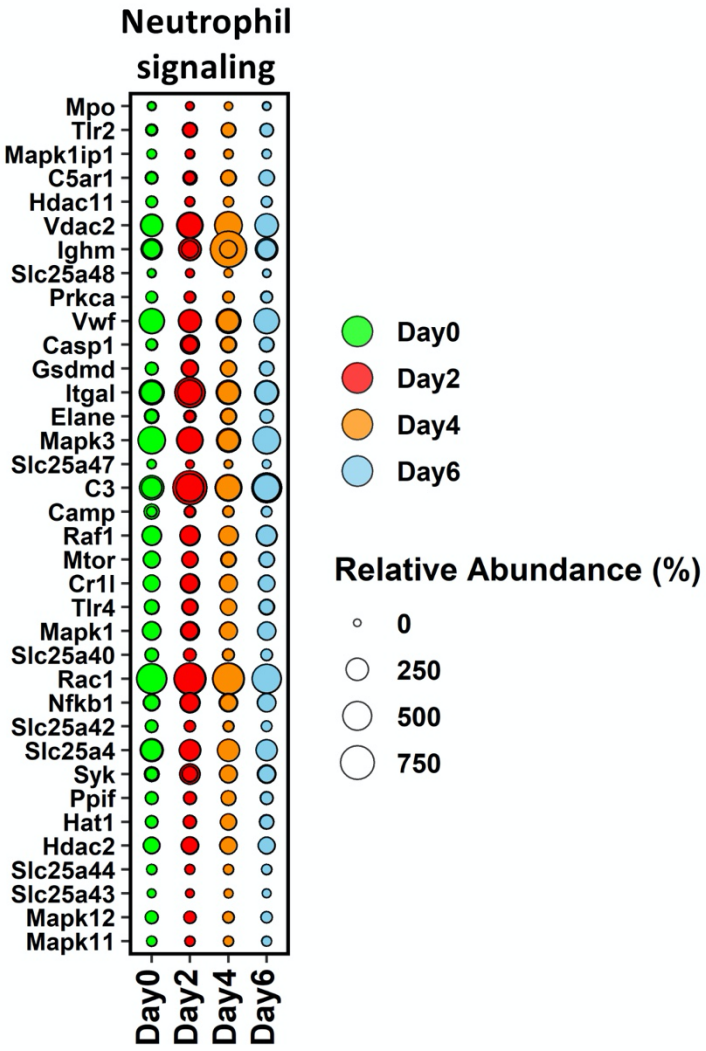

Supplemental Figure 1: Severe SARS-CoV-2 infection leads to differential expression of transcripts associated with neutrophil activity. Bubble plot of significantly changed transcripts associated with neutrophil activation and neutrophil extracellular trap formation. Bubble size denotes relative abundance and color shows time points: green (day 0, uninfected), red (day 2), orange (day 4) and blue (day 6).

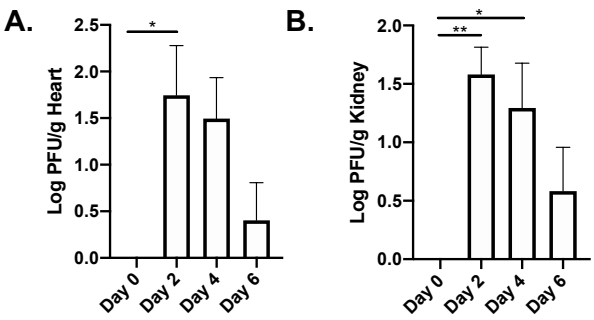

Supplemental Figure 2: Viral titers in hearts and kidneys post intratracheal challenge of golden Syrian hamsters. Male 5-to-6-week-old golden Syrian hamsters were intratracheally infected with SARS-CoV-2 strain USA-WA-1/2020 or mock challenged with vehicle (DMEM) and lungs excised at days 2, 4 and 6 post-infection. Log PFU per gram of tissue of (**A**) hearts and (**B**) kidneys assessed via plaque assays.

A.

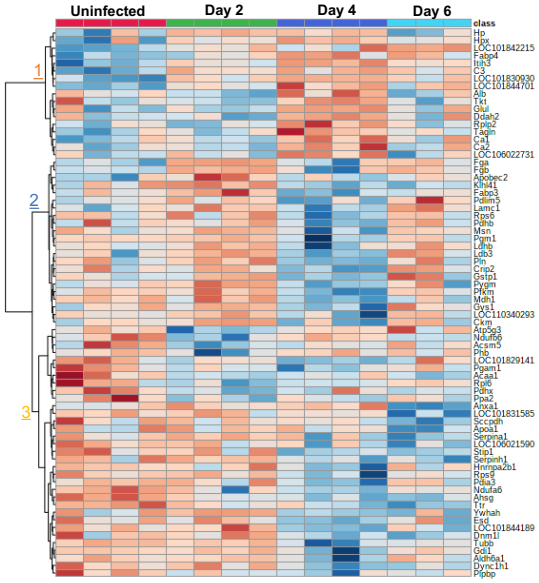

GO Terms

Cluster 1:

-aryl esterase activity
-carboxylic acid binding
-Scavenging of heme from plasma
-Binding and Uptake of Ligands by Scavenger Receptors

Cluster 2:

-NAD metabolic process
-glucose metabolic process
-energy derivation by oxidation of organic compounds
-coagulation
-homotypic cell-cell adhesion
-oxidation-reduction process
-energy reserve metabolic process
-regulation of TLR by endogenous ligand

Cluster 3:

-fatty acid metabolic process
-small molecule metabolic process
-nucleobase-containing small molecule metabolic process
-TCA cycle and respiratory electron transport
-myeloid leukocyte mediated immunity

B.

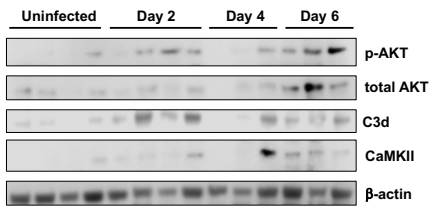

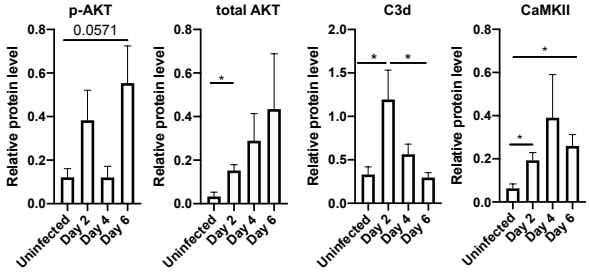

C.

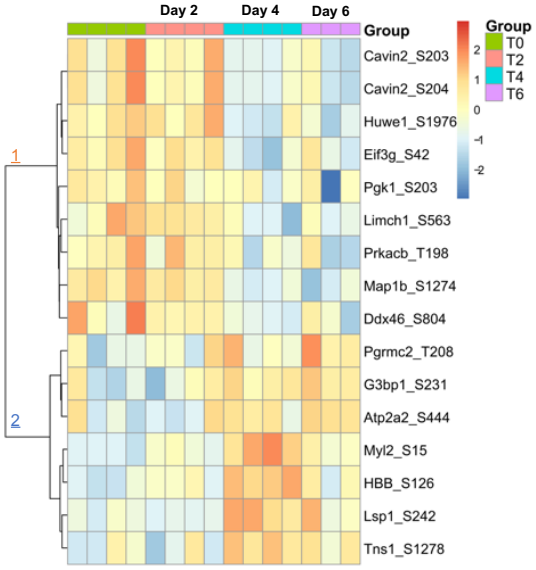

GO Terms

Cluster 1:
-cAMP-dependent protein kinase activity
-kinase activity
-cytoskeletal regulatory protein binding
-myosin II heavy chain binding
-translation initiation factor activity
-protein-disulfide reductase activity

Cluster 2:
-muscle cell fate specification
-calcium ion import into sarcoplasmic reticulum
-positive regulation of stress granule assembly
-calcium ion transport from cytosol to endoplasmic reticulum
-regulation of cardiac muscle cell action potential involved in regulation of contraction
-positive regulation of the force of heart contraction
-type I interferon production
-response to interleukin-7

Supplemental Figure 3: Severe SARS-CoV-2 leads to proteomic remodeling of hamster hearts. Male 5-to-6-week-old golden Syrian hamsters were intratracheally infected with SARS-CoV-2 strain USA-WA-1/2020 or mock challenged with vehicle (DMEM) and hearts excised at days 2, 4 and 6 post-infection. (**A**) Proteomic changes of hamster lungs after SARS-CoV-2 infection or mock challenge (n = 3-4 per timepoint). Hierarchical clustering of LFQ intensities of significantly changed proteins (ANOVA, FDR < 0.01) revealed three distinct clusters. Their abundance profiles among the groups were plotted in the heatmap. Enriched GO biological process terms are indicated for each marked cluster. (**B**) Immunoblots for complement C3d, AKT, phospho-AKT, CamKII and actin as loading control (n = 3-4 per group). Histograms of protein level quantification (densitometry). Kruskal-Wallis test with Dunn's multiple-comparison post-test. Asterisks denote the level of significance observed: * = $p \leq 0.05$. (**C**) Heatmap of phosphorylation changes of hamster kidney proteins after SARS-CoV-2 infection or mock challenge (n = 3-4 per timepoint). Hierarchical clustering of proteins with significantly changed phosphorylation state (ANOVA) revealed 2 distinct major clusters. Enriched GO biological process terms for each cluster are indicated.

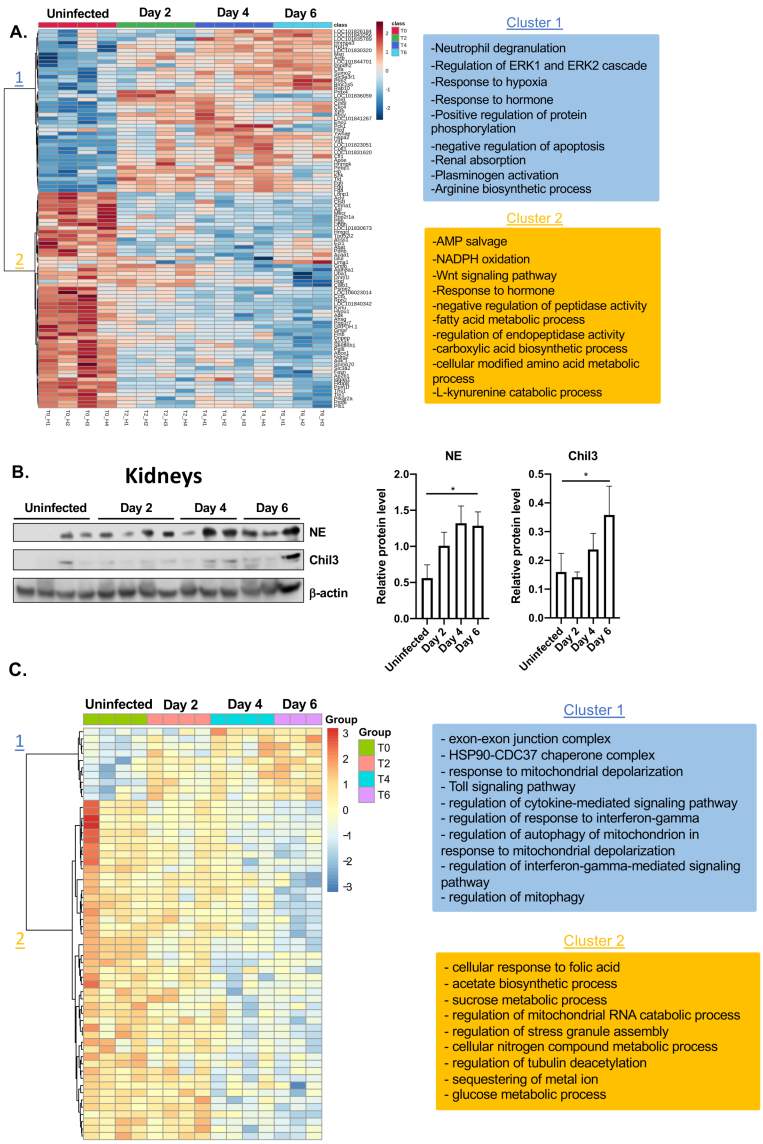

Supplemental Figure 4: SARS-CoV-2 infection leads to proteomic changes associated with tissue injury. Male 5-to-6-week-old golden Syrian hamsters were intratracheally infected with SARS-CoV-2 strain USA-WA-1/2020 or mock challenged with vehicle (DMEM) and kidneys excised at days 2, 4 and 6 post-infection. (**A**) Proteomic changes of hamster kidneys after SARS-CoV-2 infection or mock challenge (n = 3-4 per timepoint). Hierarchical clustering of LFQ intensities of significantly changed proteins (ANOVA, FDR < 0.01) revealed two distinct clusters. Their

abundance profiles among the groups were plotted in the heatmap. Enriched GO biological process terms are indicated for each marked cluster. (**B**) Immunoblots for neutrophil elastase (NE), chitinase 3 (Chil3) and actin as loading control (n = 3-4 per group). Histograms of protein level quantification (densitometry). Kruskal-Wallis test with Dunn's multiple-comparison post-test. Asterisks denote the level of significance observed: * = $p \leq 0.05$. (**C**) Phosphoproteome analysis of kidneys after SARS-CoV-2 infection reveals temporal changes to mitochondrial health and immune responses. Male 5-to-6-week-old golden Syrian hamsters were intratracheally infected with SARS-CoV-2 strain USA-WA-1/2020 or mock challenged with vehicle (PBS) and kidneys excised at days 2, 4 and 6 post-infection.

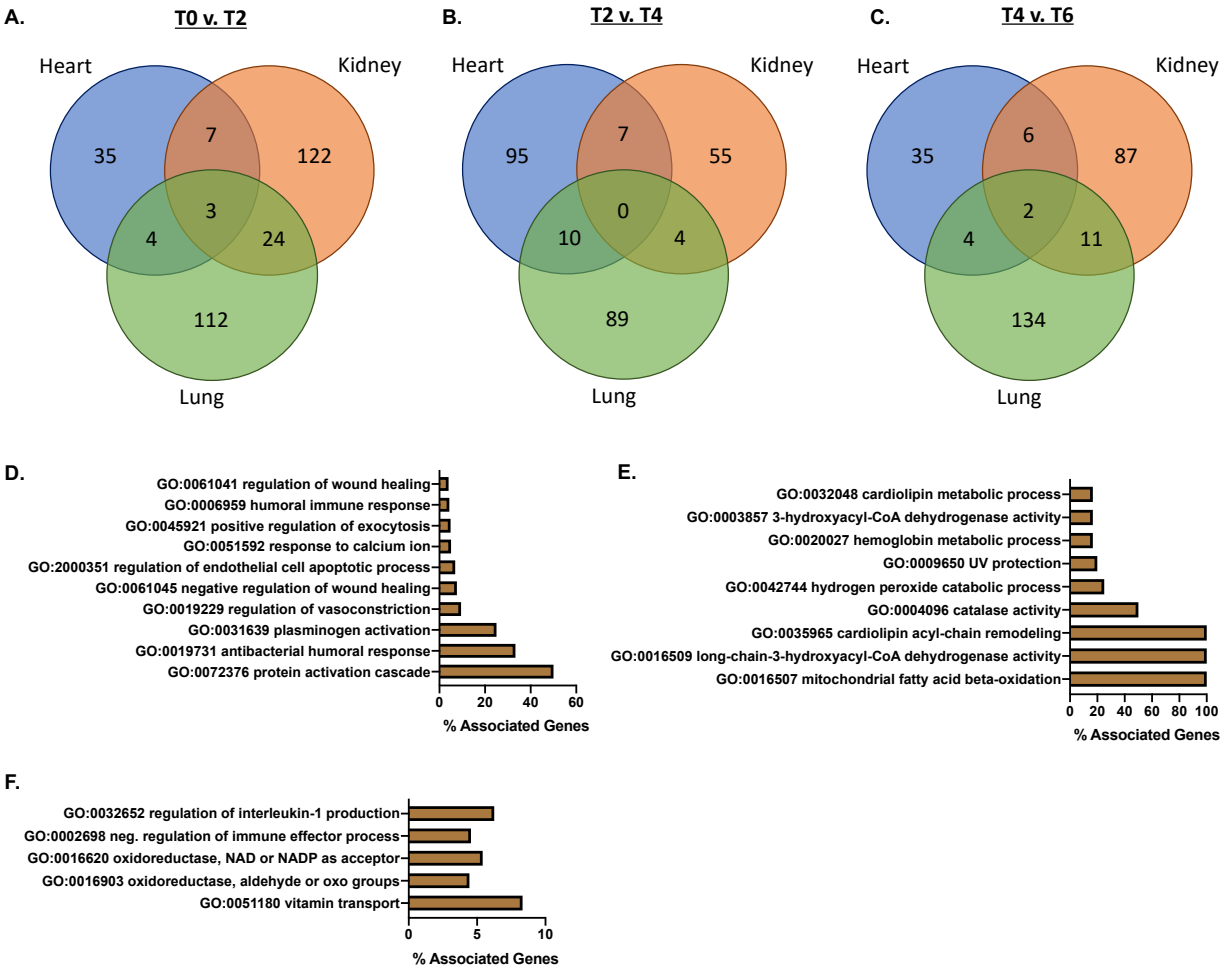

Supplemental Figure 5: Integrated kinetic multi-proteomic analysis of heart, lungs and kidneys. Venn diagram of shared proteins from global proteome analysis of lungs, hearts and kidneys at comparisons within times (**A**) T0/T2, (**B**) T2/T4 and (**C**) T4/T6. % associated genes of representative GO terms for (**D**) heart/lung/kidney at T0/T2, (**E**) heart/lung at T2/T4 and (**F**) heart/kidney/lung at T4/T6 shared factors.

Supplemental Data Set 1.

All phosphoproteins and GO terms associated with the phosphoproteome are shown.

Supplemental Data Set 2.

Full GO-term list with associated proteins and transcripts from the integrated omic analysis.

Supplemental Data Set 3.

All shared proteins and GO terms within lungs, hearts, and kidneys are presented.